Vol. 65: 103–115, 2011
doi: 10.3354/ame01536

AQUATIC MICROBIAL ECOLOGY
Aquat Microb Ecol

Published online December 13

OPEN ACCESS

FEATURE ARTICLE

Abundance of eukaryotic microbes in the deep subtropical North Atlantic

Danielle Morgan-Smith[1,*], Gerhard J. Herndl[2,3], Hendrik M. van Aken[3], Alexander B. Bochdansky[1]

[1]Department of Ocean, Earth and Atmospheric Sciences, Old Dominion University, 4600 Elkhorn Ave, Norfolk, Virginia 23529, USA

[2]Department of Marine Biology, University of Vienna, Althanstrasse 14, 1090 Vienna, Austria

[3]Royal Netherlands Institute for Sea Research, PO Box 59, 1790 AB Den Burg (Texel), The Netherlands

ABSTRACT: The meso- and bathypelagic ocean comprises the largest habitat on earth, yet we know very little about the distribution and activity of protists in this environment. These small eukaryotes are responsible for controlling bacterial abundance in the surface ocean and are major players in the material and energy transfer of pelagic food webs. In this paper, we quantify microbial eukaryotes in the deep North Atlantic, as well as provide a basic characterization of eukaryote community changes through the water column. To this end, we counted organisms using 2 different approaches: (1) catalyzed reporter deposition fluorescence *in situ* hybridization (CARD-FISH, also known as TSA-FISH) with the EUK516 probe and the newly developed KIN516 probe for kinetoplastids, and (2) 4′,6-diamidino-2-phenylindole in combination with fluorescein isothiocyanate staining (DAPI-FITC). We performed several tests to compare the abundances measured by these 2 methods, and quantified losses at each step in the process. We also used the morphology of nuclei stained with DAPI as a quick method to characterize some groups of protists. We found that eukaryotes and kinetoplastids both decreased in abundance with increasing depth at a greater rate than bacteria or viruses. Below 1000 m and to the maximum depth collected in this study (i.e. 5000 m) the concentration of eukaryotic microbes counted using both methods remained constant. Kinetoplastids represented a significant fraction (average 21.8%) of total eukaryotic microbes counted by CARD-FISH throughout the water column, and this percentage increased somewhat with depth. One unique yet unidentified nuclear morphotype as identified by DAPI staining remained equally abundant throughout the entire water column, and was the most abundant protist in deep-sea samples.

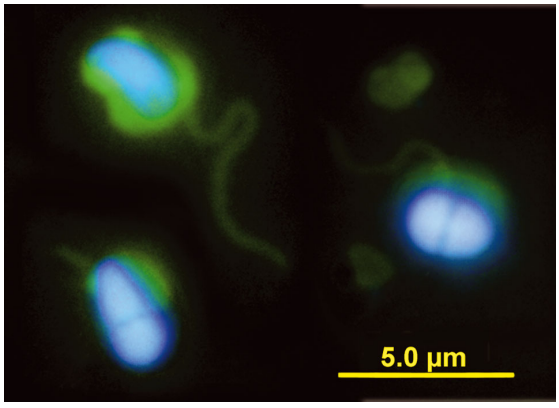

Bathypelagic eukaryotes with DAPI-FITC staining. The 2 lower cells are of the split-nucleus morphotype which dominated deep-water samples.

Image: D. Morgan-Smith

KEY WORDS: Eukaryotic microbes · Deep sea · CARD-FISH

INTRODUCTION

The deep sea is the largest habitat on Earth, but is still relatively unexplored with respect to microbiology due to the difficulty of sampling such a distant and sparsely inhabited environment. In particular, small eukaryotes have only been examined and enumerated at depths below 1000 m in a few studies (Patterson et al. 1993, Tanaka & Rassoulzadegan 2002, Countway et al. 2007, Fukuda et al. 2007, Sohrin et al. 2010). In the surface ocean, heterotrophic nanoflagellate abundances are 10^2 to 10^4 cells ml^{-1} and bacterial

*Email: dmorgan@odu.edu

abundances are 10^5 to 10^7 cells ml^{-1} (Gasol & Vaque 1993), and flagellates are known to control bacterial densities through grazing (Fenchel 1986). Whereas in the mesopelagic flagellates may still be important grazers on bacteria (Fukuda et al. 2007), they may play a less important role in the bathypelagic environment (Aristegui et al. 2009).

Based on 18S rRNA sequences, Countway et al. (2007) found protistan communities in the deep sea distinct from those in the surface ocean. Fukuda et al. (2007) found that biomass of eukaryotic microbes dropped off more sharply with depth than prokaryotic biomass. In another study, a large diversity of diplonemids was reported in the deep sea (Lara et al. 2009). A recent review of deep-sea microbial oceanography included a comparison of eukaryote numbers between the Pacific and Atlantic Oceans, and the Mediterranean Sea (Aristegui et al. 2009). Most recently, protist numbers were reported for a large longitudinal transect from 10° S to 53° N at depths of 5 to 5000 m in the Pacific Ocean (Sohrin et al. 2010), and protist diversity in the deep, anoxic Cariaco Basin was reported (Edgcomb et al. 2011). Of the many available methods, only direct counts yield absolute numbers of protists in water samples, which is a critical piece of information to better understand microbial trophodynamics. Using samples collected on the same cruise used in the present study, Parada et al. (2007) found that abundances of picoplankton decreased exponentially from about 2.9×10^5 cells ml^{-1} at 100 m to 0.2×10^5 cells ml^{-1} at 4000 m. One may thus hypothesize that flagellates do not thrive in the deep sea because the abundance of prokaryote prey falls below their feeding threshold (ca. 10^5 cells ml^{-1}; Andersen & Fenchel 1985, Wikner & Hagström 1991), and that viruses, which maintain very high concentrations in the deep sea (Parada et al. 2007), are more likely to control prokaryotic abundance in deep water.

Three stains have been commonly used to obtain nanoflagellate counts in the ocean. These are 4′,6-diamidino-2-phenylindole (DAPI), fluorescein isothiocyanate (FITC), and 3-6-diamino-acridine hemisulfate (Proflavine). Of these, DAPI stains the nucleus only, and is used in combination with FITC (Paffenhöfer et al. 2003, Fukuda et al. 2007) or Proflavine (Tanaka & Rassoulzadegan 2002), which stain the entire cell body. Here we report cell abundances based on conventional DAPI-FITC staining and compare them with catalyzed reporter deposition fluorescence *in situ* hybridization (CARD-FISH; Beardsley et al. 2005) based on a probe considered universal to eukaryotes.

MATERIALS AND METHODS

Sample collection

Water samples of 200 to 1250 ml were collected using Niskin bottles from 17 stations in the North Atlantic during the ARCHIMEDES-I cruise (Fig. 1) between November 13 and December 9, 2005. Samples were taken at depths of 100 to 5000 m, with most stations sampled at 900, 2750, and 4000 m, representing Antarctic Intermediate Water, North Atlantic Deep Water, and Antarctic Bottom Water, respectively (Tomczak & Godfrey 2003). Samples were fixed overnight in formaldehyde (2% final concentration, stabilized with methanol), then filtered onto 0.2 or 0.8 µm pore size white polycarbonate filters (Millipore GTTP and ATTP, respectively) at a vacuum of −200 mbar. The relatively long fixation at room temperature was necessary so that supersaturated gases were able to escape and thus not form bubbles on the filters, which would lead to non-uniform cell distributions. Filters were rinsed twice with 1× phosphate buffered saline (PBS), then with MilliQ water and immediately frozen at −80°C. They were transported from the Netherlands to Norfolk on dry ice via courier and subsequently stored in a −80°C freezer until CARD-FISH or direct staining was performed.

CARD-FISH

Prior to hybridization, pie-shaped pieces of approximately 1/8 filter were cut so that multiple analyses could be run on a single filter representing a single water sample. The CARD-FISH protocol (Pernthaler et al. 2002, Teira et al. 2004) was undertaken on each filter section, with 10 to 12 sections hybridized simultaneously from various filters. Filter sections were embedded in warm 0.1% agarose to prevent cells from detaching from the filters during the hybridization and washing procedures. Permeabilization steps common for FISH with prokaryotes (Proteinase K or lysozyme treatment) were not used as they would damage the more fragile protist cell bodies. Probes labeled with horseradish peroxidase (HRP) were EUK516 (Amann et al. 1990) and KIN516 (Bochdansky & Huang 2010) (Table 1), and competitor probes (probes not labeled with HRP displaying one central mismatch with the active probe, Table 1) were used for all hybridizations except for the depressurization tests (see 'Effects of depressurization' below).

Hybridization took place at 35°C for 14 to 17 h in hybridization buffer containing 55% formamide (1 g

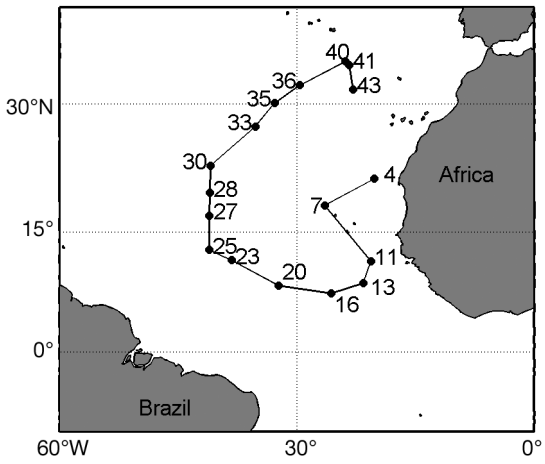

Fig. 1. Stations sampled in the North Atlantic. Station numbers are the same as in Parada et al. (2007). Stations along the western portion of the cruise track followed the North Atlantic Deep Water along the Mid Atlantic Ridge

dextran sulfate, 1.8 ml 5 M NaCl, 200 µl 1 M Tris-HCl, 5 µl 100% Triton X-100, 5.5 ml formamide, 1 ml 10% blocking reagent, 1.5 ml Barnstead Nanopure water). Filters were then washed with washing buffer (30 µl 5 M NaCl, 1 ml 1 M Tris-HCl, 500 µl 0.5 M EDTA, 50 µl 10% sodium dodecyl sulphate [SDS], brought to 50 ml with Barnstead Nanopure water) for 15 min at 37°C, followed by PBS-T solution (5 ml 10× PBS, 25 µl Triton X-100, brought to 50 ml with Barnstead Nanopure water) for 10 min at room temperature. Amplification was performed at 37°C for 15 min in the dark in amplification substrate B (493 µl amplification buffer, 5 µl Alexafluor 488, 5 µl amplification substrate A; amplification buffer: 2 g dextran sulfate, 8 ml 5 M NaCl, 200 µl 10% blocking reagent, 11.8 ml 1× PBS; amplification substrate A: 1 µl H_2O_2, 200 µl amplification buffer), then washed at room temperature in PBS-T solution for 10 min in the dark. After CARD-FISH, filters were mounted individually on microscope slides using Vectashield liquid mounting medium with DAPI as counter-stain, and stored horizontally at −20°C in the dark.

Table 1. The 2 horseradish peroxidase (HRP)-labeled probes (Beardsley et al. 2005) used in this study. As there is only one central mismatch (**bold**, underlined), unlabeled sequences of each probe were used as competitor probes to increase discriminatory power

Name	Sequence	Source
EUK516	5′-ACC AGA CTT G**C**C CTC C-3′	Amann et al. (1990), Beardsley et al. (2005)
KIN516	5′-ACC AGA CTT G**T**C CTC C-3′	Bochdansky & Huang (2010)

Robotic microscopy

Samples were analyzed on a modified Olympus BX51 epifluorescence microscope with computer control of the stage in *X*, *Y*, and *Z* planes using a motorized stage with linear encoding (Prior Scientific). An X-Cite 120 (Exfo) light source provided highly consistent illumination. Band-pass filters (40 nm band at 360 nm, 15 nm band at 484 nm, and 25 nm band at 555 nm; Chroma Technology) in a Lambda 10-3 filter wheel (Sutter Instrument) along with a multi-band beamsplitter (61000v2bs, Chroma Technology) and emission filter (20 nm band at 450 nm, 35 nm band at 520 nm, 45 nm band at 605 nm; 61000v2m, Chroma Technology) allowed scanning of the slide for both DAPI and the hybridization signal, with automatic shutters switching between the 2 excitation wavelengths at each image field. Images were taken with a QICam Fast 1394 (Qimaging) cooled charge-coupled device camera. Microscope control and image acquisition were performed with Objective Imaging software in combination with Image-Pro Plus software with customized macros for microscope operation.

Filter slices were scanned using a semi-automated process. First, the entire filter area was scanned in brightfield illumination at 40× total magnification. This allowed the area of the filter to be defined within the Image-Pro software as a custom scan area. The *Z*-stack for the scan was defined by noting the *Z*-plane of best focus for several points on the filter and setting a *Z*-range based on those values. The filter area was then scanned at 400× using the automated stage and the resulting images stitched into a mosaic of approximately 300 to 600 fields for display in Image-Pro, with images from the blue and green emission channels overlaid to create a single false-colored image on-screen. The *Z*-stack for each image in the mosaic, consisting of approximately 30 to 50 images for each stack, was assembled using an algorithm which combined areas of greatest contrast, to create focus across each image and the entire mosaic. The coordinates of each image pixel were stored so that the operator was able to return to any location on the filter to re-examine specific organisms and to take additional pictures at higher magnification. Organisms with positive hybridization signals as well as DAPI-stained nuclei were identified, counted, and individually photographed at 1000× total magnification in each channel.

These photographs were sorted based on the morphotype of the nucleus in DAPI. Depending on the abundance of organisms in the sample, 5 to 446 protists were counted per sample using EUK516, and 0 to 232 kinetoplastids were counted using KIN516.

Nuclear morphology

Nuclear morphological categories as they appeared in DAPI were defined as 'crescent', 'long' (longest dimension at least 3 times greater than the shortest dimension), 'kinetoplastid' (nucleus coupled with a distinctive kinetoplast), 'donut' (round nucleus with a dark center), 'bean' (one convex and one concave side), 'split' (round nucleus with a distinctive dark line down the center), 'round', and 'miscellaneous' (all nuclei that do not fit into any of these groups). Fig. 2 shows examples for each of these morphotypes.

Effect of depressurization

This experiment was designed to determine whether there were any pre-fixation losses of cell numbers while the water samples were raised through the water column. Samples were collected from 2750 and 4000 m depths at 6 stations in four 200 ml titanium chambers designed to retain *in situ* pressure. Pressure was released in 2 of the chambers before fixation with formaldehyde (2% final conc.). In the 2 other chambers, formaldehyde (2% final conc.) was injected through a high pressure liquid chromatography pump (Rainin Instrument) without loss of pressure. After 0.5 h of fixation to cross-link proteins and thus harden cells, pressure was released. All samples were filtered through 0.2 µm Millipore polycarbonate filters and hybridized with the EUK516 probe as described in 'CARD-FISH' above, but without the use of a competitor probe.

Methodological tests

In order to assess a variety of potential sources of error, we performed a series of tests. We quantified each of them separately, then arrived at an overall correction factor. In this fashion, our results can be compared with many different methods and protocols employed in other studies.

Prokaryotes on hybridized and unhybridized filters. To determine whether material was lost from the filter surface during the hybridization procedure, 1/8 slices of 25 mm, 0.8 µm pore size polycarbonate filters were hybridized with the EUK516 or KIN516 probe, counterstained with DAPI and then analyzed under epifluorescence microscopy for DAPI signals of prokaryotes. These counts were compared with counts taken from 1/8 sections of the same filter stained with DAPI and not put through hybridization.

Pore size comparison. In order to determine whether any eukaryotic microbes were lost through the pores of the 0.8 µm pore-size filters, paired deep-sea samples taken from a single Niskin bottle at each of 8 stations were formaldehyde-fixed and filtered through 0.2 and 0.8 µm pore size polycarbonate filters at a vacuum of 200 mbar. Sample volumes were 250 ml for the 0.2 µm filters and 1000 ml for the 0.8 µm filters. Filters were stored at −80°C and 1/8 (for 0.8 µm) or 1/4 (for 0.2 µm, the larger portion necessary to count sufficient organisms

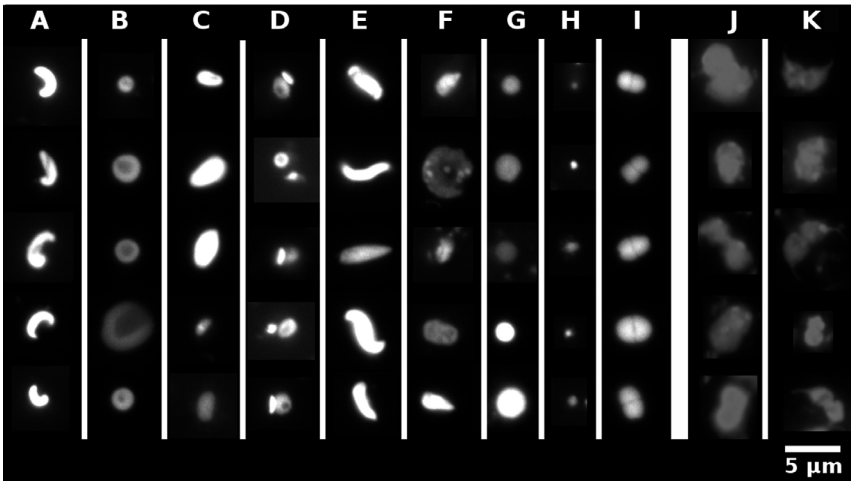

Fig 2. (A–I) 5 examples for each of the nuclear morphotypes. (A) Crescent, (B) donut, (C) bean, (D) kinetoplastid (with the characteristically large mitochondrion), (E) long, (F) miscellaneous (non-round), (G) round, (H) tiny, and (I) split. All photos show DAPI-stained nuclei of organisms from the deep sea with positive EUK516 hybridization, except for the kinetoplast morphotype, which were all positive with the KIN516 probe. (J, K) Examples of cultured diplomonads: 2 known organisms with double nuclei for comparison with the split nucleus morphotype. (J) *Hexamita pusilla* ATTC #50336, (K) *Trepomonas agilis* ATTC #50337

given the smaller volume filtered) of the filter was mounted on a slide using Vectashield with DAPI mounting medium and counted using epifluorescence microscopy.

Test for detachment of organisms from filters. The purpose of this test was to determine whether material would fall off the filters during shipping and storage. A culture of *Cafeteria roenbergensis* was fixed with 2% formaldehyde and 10 ml aliquots were filtered through 0.8 µm pore size polycarbonate filters. Five such filters were placed gently into PetriSlides (Millipore) and stored at −80°C for 1 wk. The other 5 filters were placed into PetriSlides, then shaken vigorously, and knocked against the surface of the lab bench. These filters were then stored at −80°C in the PetriSlides, removed several times to be shaken and dropped on the lab bench to simulate handling rougher than occurred with the deep-sea samples. At the end of 1 wk, all filters were allowed to thaw and were then mounted on slides using Vectashield with DAPI mounting medium and counted using epifluorescence microscopy.

DAPI-FITC staining test. In order to compare the efficiency of DAPI and FITC staining procedures with each other, slices of 1/8 of a filter of cultured flagellates (*Neobodo designis, Paraphysomonas vestita,* and *Cafeteria roenbergensis*) were embedded in agarose, as in the CARD-FISH protocol, then soaked for 10 min in 30% H_2O_2 to reduce background fluorescence. Filters were then soaked in FITC solution (2.5 ml sodium carbonate buffer, pH 9.5; 11 ml potassium phosphate buffer, pH 7.2; 11 ml 0.85% NaCl; 10 mg FITC) for 10 min, and washed in sodium carbonate buffer (pH 9.5) for 20 min. Filter slices were mounted on microscope slides and counterstained using Vectashield with DAPI mounting medium. This FITC staining procedure was not performed on deep-sea samples, only on cultured flagellates, and differs somewhat from the method used for deep-sea samples. Organisms were counted first in UV excitation for DAPI only, then in DAPI-FITC (i.e. a positive signal in both color channels was required for an organism to be counted).

DAPI versus EUK516+KIN516 in lagoon samples. Samples of ambient water, marine snow particles, and sediment were collected in Carrie Bow Cay, Belize, formaldehyde fixed and filtered through 0.8 µm pore size polycarbonate filters. Sections of 1/8 filter each were hybridized with EUK516 and KIN516 probes. All filters were mounted on slides using Vectashield with DAPI mounting medium. Epifluorescence counts were done first counting protists in DAPI only, then counting organisms with both a positive hybridization signal and a visible nucleus in DAPI. This test was designed to account for organisms whose sequences do not match that of either probe. Details of this test can be found in Bochdansky & Huang (2010).

Manual counts. Slices of 1/8 filter mounted in Vectashield with DAPI medium were first counted robotically (see 'Robotic microscopy' above), and then later recounted using the same microscope described in 'Robotic microscopy' but with manual control of the stage without the aid of camera and imaging software over a minimum of 200 fields. This was performed on all CARD-FISH samples to assess whether the robotic scanning process introduces error.

DAPI-FITC counts. Sections of 1/8 of a 0.8 µm pore size polycarbonate membrane filter were taken from the same filters used for CARD-FISH. These were placed on top of a 3.0 µm pore size polycarbonate membrane backing filter on a glass filtration tower. The filter slices were flooded with 1 ml of FITC staining solution (10 mg FITC, 11 ml potassium phosphate buffer, 11 ml 0.85% NaCl, 2.5 ml sodium carbonate buffer; Sherr & Sherr 1983). After 10 min of incubation in the dark, vacuum was applied to remove staining solution, then filters were rinsed twice with 10 ml cold (4°C) sodium carbonate buffer under ~200 mbar vacuum. Filters were mounted on slides using Vectashield with DAPI mounting medium, and stored at −20°C in the dark until they were counted on an Olympus BX50 epifluorescence microscope.

Prokaryotic size spectrum

To obtain prokaryotic counts, we scanned a random pattern of at least 100 fields per filter section at 1000× total magnification. This was performed on 0.2 µm pore size membrane filters from all stations. Minimum size and intensity cutoffs were set based on which objects appeared to be prokaryotes (i.e. those that would be counted as prokaryotes in DAPI), and image analysis was run using Image-Pro Plus to count such objects in each field. Concentrations of prokaryotes (cells ml^{-1}) were then calculated, accounting for the volume of water filtered and the proportion of the total filter area included in the scanned region.

Statistical analyses

Pearson correlation analyses were conducted to compare biological and environmental parameters,

including total eukaryote, kinetoplastid and split nucleus abundances by CARD-FISH, depth, latitude, longitude, distance to nearest land, and measured nitrogen and phosphorus species. Pearson correlation analyses were also used to compare prokaryotic abundances obtained using image analysis to CARD-FISH abundances of total eukaryotes, kinetoplastids and the split nucleus organism. Linear regression of kinetoplastid abundance and kinetoplastids as a percentage of total CARD-FISH eukaryotes against depth were performed. Paired *t*-tests and Wilcoxon signed rank tests were conducted on groups 1, 2, 4, 5, 6, 7, and 8 of the methodological tests (Table 2). Student's *t*-tests and Wilcoxon rank sum tests were used for group 3, which did not have paired samples. All tests were performed using Matlab Statistics Toolbox.

RESULTS

Abundances of eukaryotes counted using DAPI-FITC staining were an average of 228 cells ml^{-1} (SD = 248) in samples from the lower part of the euphotic zone (100 m), 25.7 cells ml^{-1} (SD = 19.6) in the Antarctic Intermediate Water (750–1000 m), 11.2 cells ml^{-1} (SD = 5.7) in the North Atlantic Deep Water (2400–2750 m), and 12.1 cells ml^{-1} (SD = 7.3) in the Antarctic Bottom Water (3500–5000 m) (Fig. 3D). DAPI-FITC eukaryote abundance was significantly higher in the central water (100–500 m) than in any of the lower water masses (Table 3), none of which were significantly different (1-way ANOVA with Tukey-Kramer multiple comparison correction, $p < 0.0001$, $F = 9.91$). Similarly, we found that overall eukaryote abundances counted by CARD-FISH decrea-

Table 2. Results of statistics for methodological tests. **Bold** numbers indicate significant results at the $\alpha = 0.05$ level. Since the assumptions of parametric tests were not always fulfilled, the results of the non-parametric equivalents are shown as well. For test group 3 an unpaired Student's *t*-test and Wilcoxon rank sum test were used; for all other groups, paired Student's *t*-tests and Wilcoxon signed rank tests were performed. Group 1: counts of prokaryotes (Prok.) in DAPI on hybridized versus unhybridized deep-sea filters. Group 2: eukaryotes (Euk.) counted in DAPI on 0.2 µm versus 0.8 µm pore size deep-sea filters. Group 3: counts in DAPI of cultured *Cafeteria roenbergensis* (*Caf.*) on filters subjected to shaking versus filters which were left undisturbed. Group 4: eukaryotes counted in CARD-FISH on deep-sea samples maintained at *in situ* pressure until after fixation versus samples depressurized prior to fixation. Group 5: counts of several flagellate cultures using DAPI versus DAPI-FITC staining techniques. Group 6: eukaryotes from ambient and untreated lagoon waters of Carrie Bow Cay, Belize, counted in DAPI versus using CARD-FISH (details in Bochdansky & Huang 2010). Group 7: counts of the same deep-sea filter slices hybridized with the EUK516 and KIN516 probe pair using robotic versus manual control of the microscope stage. Group 8: deep-sea samples using CARD-FISH with the EUK516 and KIN516 probe pair versus counts on different sections of the same filter using DAPI-FITC staining. DAPI: 4′,6-diamidino-2-phenylindole staining; FITC: fluorescein isothiocyanate staining; CARD-FISH: catalyzed reporter deposition fluorescence *in situ* hybridization

Test group	Mean (cells ml^{-1})	SD (cells ml^{-1})	n	*t*	p	Rank sum/ signed rank	p
1a. Prok. on hyb. filters	38775	20629	58	**11.3**	**<0.0001**	**5**	**<0.0001**
1b. Prok. on fresh filters	50828	25098	58				
2a. Euk. on 0.2 µm filters	37.1	16.6	8	**4.06**	**0.0048**	**0**	**0.0078**
2b. Euk. on 0.8 µm filters	26.5	10.9	8				
3a. *Caf.* on shaken filters	10964	1081	5	–0.409	0.703	28	>0.999
3b. *Caf.* on unshaken filters	11022	998	5				
4a. Pressurized samples	1.06	0.815	14	0.986	0.342	36	0.326
4b. Depressurized samples	0.782	0.554	14				
5a. Cultures in DAPI-FITC	6884	7649	12	0.381	0.710	33	0.677
5b. Cultures in DAPI	6666	6993	12				
6a. Protists in DAPI	1594	1195	11	**6.28**	**<0.0001**	**0**	**0.0009**
6b. EUK516+KIN516	1236	1327	11				
7a. EUK+KIN robotic	10.5	26.2	60	**–3.75**	**0.0004**	**109**	**<0.0001**
7b. EUK+KIN manual	15.8	32.8	60				
8a. Deep-sea EUK+KIN	15.9	33.3	58	**3.50**	**0.0009**	**0**	**<0.0001**
8b. Deep-sea DAPI-FITC	77.9	163.8	58				

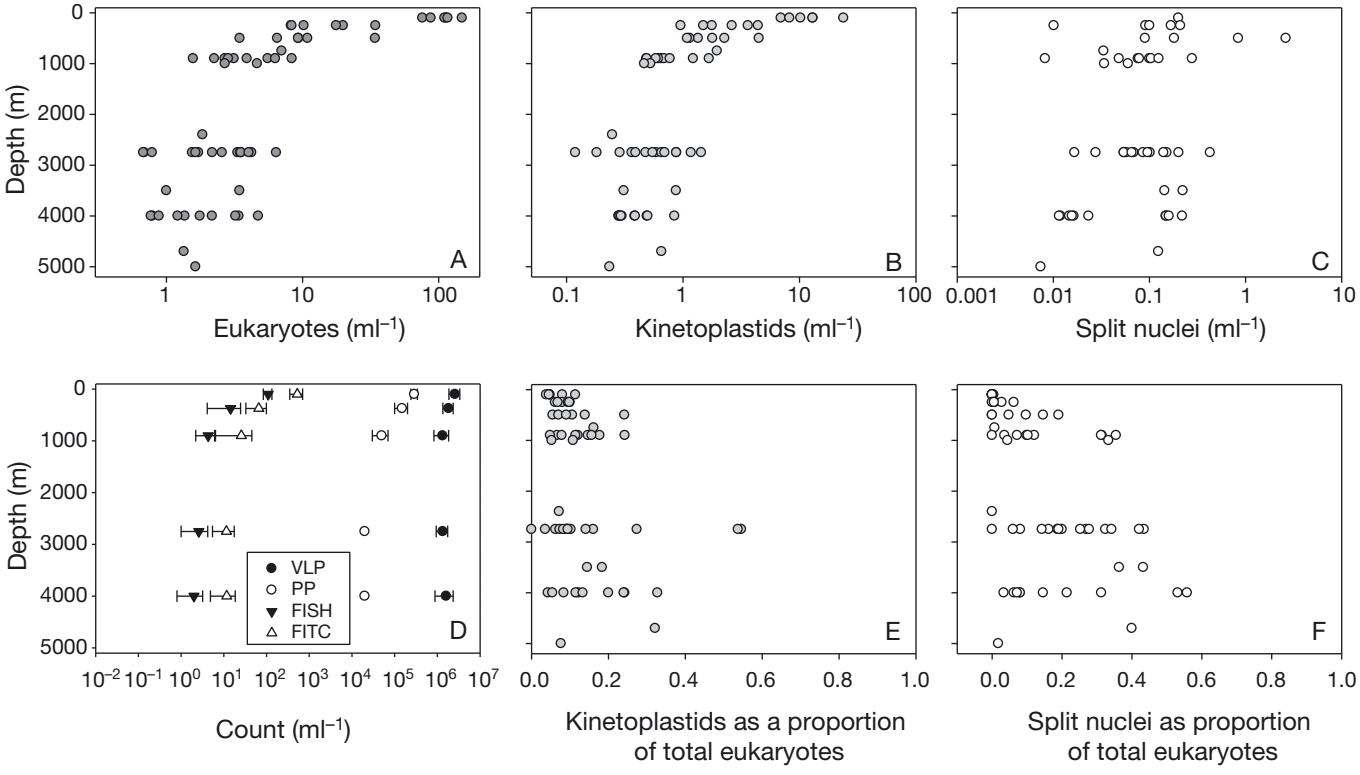

Fig 3. (A–C) Counts in cells ml^{-1} of eukaryotes (EUK516 + KIN516 probes), kinetoplastids (KIN516 probe) and split nucleus (based on morphology), respectively. (D) Mean values of virus-like particle (VLP), picoplankton (PP), CARD-FISH (FISH) eukaryote, and DAPI-FITC (FITC) eukaryote abundances. Error bars represent SD over the depths sampled. VLP abundances remain within a factor of 2, PP decrease by about an order of magnitude, and eukaryotes decrease by about 2 orders of magnitude with both methods. VLP and PP from Parada et al. (2007). (E, F) Kinetoplastids and the split nuclear morphotype as a proportion of total eukaryotes (EUK516 + KIN516), respectively. All eukaryote and kinetoplastid graphs based on manually counted CARD-FISH samples, except FITC portion of (D). Split nucleus abundance in (C) and (F) are based on morphology observed in robotically counted samples. DAPI-FITC: 4′,6-diamidino-2-phenylindole and fluorescein isothiocyanate staining; CARD-FISH: catalyzed reporter deposition fluorescence *in situ* hybridization

Table 3. Mean (range) of eukaryote abundances measured at various depth ranges (in cells ml^{-1}). Columns 2 to 4 show data from the present study, counted manually in CARD-FISH (catalyzed reporter deposition fluorescence *in situ* hybridization) and in DAPI-FITC (4′,6-diamidino-2-phenylindole and fluorescein isothiocyanate staining) as described in 'Materials and methods'. The last 4 columns show results from previous studies which used DAPI and FITC staining (Fukuda et al. 2007, Sohrin et al. 2010), DAPI and Proflavine (Tanaka & Rassoulzadegan 2002) or live counts (Patterson et al. 1993). Data from Tanaka & Rassoulzadegan (2002) and Patterson et al. (1993) are estimated visually from published figures. Samples were taken at different depths within the given ranges in each study. The values shown for Fukuda are medians for samples taken at 10 m, 100–1000 m, and 1000–3750 m

Depth (m)	DAPI-FITC	FISH robotic	FISH manual	Fukuda	Sohrin	Tanaka	Patterson
0–100				1400 (180–3300)	316 (210–738)	300 (20–900)	
100–110	525 (269–725)	82 (47–111)	109 (76–149)		218 (177–262)	60 (13–170)	60
200–250	89 (48–145)	12 (1.7–46)	16 (8.2–34)		42 (29–57)	25 (17–30)	60
500	47 (27–68)	6.3 (0.44–28)	12 (3.5–34)	60 (5.7–260)	20 (12–24)	15 (6–20)	10
750–1000	26 (6.6–82)	1.2 (0.09–4.8)	4.3 (1.6–8.4)		13 (10–19)	5 (2.5–10)	10
1500–3500	12 (6.5–31)	0.50 (0.04–1.8)	2.6 (0.68–6.4)	6.6 (1.4–12)	8.9 (6.2–12)	2 (1.1–8)	20
3500–5000	12 (6.4–32)	0.40 (0.16–1.1)	2.0 (0.77–4.7)		8.8 (5.5–9.9)		

sed sharply from a mean of 109 cells ml^{-1} (SD = 25, range = 76 to 149, n = 6) in samples from the lower part of the euphotic zone (100 m) to 4.3 cells ml^{-1} (SD = 2.1, range = 1.6 to 8.4, n = 12) in the Antarctic Intermediate Water (750–1000 m), then remained fairly constant through the North Atlantic Deep Water (2400–2750 m) with a mean of 2.6 cells ml^{-1} (SD = 1.6, range = 0.68 to 6.4, n = 16), and the Antarctic Bottom Water (3500–5000 m) with a mean of 2.0 cells ml^{-1} (SD = 1.2, range = 0.77 to 4.7, n = 14) (Fig. 3). Eukaryote distribution was strongly correlated with depth and therefore with other factors that were strongly depth-dependent, such as nutrient concentrations (Table 4). The same trends held for kinetoplastids, but not for the split-nucleus morphotype, which was not significantly correlated with depth or nutrients. No significant correlations existed with latitude, longitude, or distance to nearest land for any group (Table 4).

Because of an apparent discrepancy between counts obtained by DAPI-FITC and CARD-FISH methods, we undertook the series of methodological tests described in 'Methodological tests' above. These tests led us to several sources of error potentially accounting for the discrepancy observed; these sources are summarized in Table 2. Significant differences were found in groups 1, 2, 6, and 7 (i.e. losses due to hybridization procedure, filter pore size, staining method, and robotic control of the microscope stage, respectively). These comparisons all showed that CARD-FISH with robotic microscopy underestimated protist abundance, counting 76.3, 71.4, 76.1, and 66.7%, respectively, of the organisms compared to the control, for groups 1, 2, 6, and 7, respectively. Compounding the errors for the 4 factors tested in these groups, the CARD-FISH method should count 38.7% of protists in a sample, a 2.6-fold difference on average compared with DAPI-FITC. This is approximately half of the 4.9-fold overall difference between the 2 methods, comparing DAPI-FITC and CARD-FISH estimates of eukaryotes in deep-sea samples (group 8, Table 2). Factors that we tested and that did not contribute to the observed discrepancies were detachment of cells from filters (group 3), depressurization of samples before fixation (group 4), and differences between independent DAPI and DAPI-FITC counts (group 5) (Table 2). Factors we did not investigate, but which could contribute to the other half of the discrepancy observed, include differences in the rRNA and protein content of eukaryotic cells, counting of dead eukaryotic cells, or inclusion of some large prokaryotes in the DAPI-FITC counts.

Based on manual CARD-FISH counts, kinetoplastid abundance averages were 5.7 cells ml^{-1} (SD = 6.1) in the upper water column (100–500 m), dropping off sharply to 0.84 cells ml^{-1} (SD = 0.50) in the Antarctic Intermediate Water, 0.56 cells ml^{-1} (SD = 0.39) in the North Atlantic Deep Water, and 0.44 cells ml^{-1} (SD = 0.21) in the Antarctic Bottom Water. Using the empirical correction factor of 4.9 as assessed above, corrected kinetoplastid abundances were 27.9 cells ml^{-1} for 100–500 m, 4.1 cells ml^{-1} for the Antarctic Intermediate Water, 2.7 cells ml^{-1} for the North Atlantic Deep Water, and 2.2 cells ml^{-1} for the Antarctic Bottom Water. The abundance of kinetoplastids decreased significantly with depth (linear regression on semi-log transformed data, Fig. 3; $F = 106$, $p < 0.0001$, n = 60). As a percentage of total CARD-FISH eukaryotes, however, kinetoplastids increased with depth (linear regression on semi-log transformed data, Fig. 3; $F = 5.87$, $p = 0.019$, n = 60). Kinetoplastid percentage averages of total eukaryotic microbes were 15.9% (SD = 7.4) at 100–500 m, 21.5% (SD = 9.0) in the Antarctic Intermediate Water, 24.0% (SD = 20.3) in the North Atlantic Deep Water, and 27.1% (SD = 13.3) in the Antarctic Bottom Water.

Community composition based on nuclear morphotype changed with depth. Images of DAPI-stained nuclei for all FISH-positive organisms were sorted into 9 categories and labeled

Table 4. Pearson correlation coefficients (r) between cell abundances (cells ml^{-1}) measured by manual counting of CARD-FISH samples and geographic and chemical variables, with corresponding p-values, n = 57. NO_x = NO_2 + NO_3, TP = total phosphorus, TN = total nitrogen

Variable	Eukaryotes		Kinetoplastids		Split nuclei	
	r	p	r	p	r	p
Depth (m)	−0.487	<0.0001	−0.474	0.0001	−0.135	0.318
Latitude (°N)	0.223	0.086	0.233	0.073	0.068	0.617
Longitude (°W)	−0.003	0.981	0.008	0.954	−0.049	0.717
Distance to nearest land (km)	−0.047	0.724	−0.062	0.639	−0.019	0.886
PO_4 (µmol ml^{-1})	−0.704	<0.0001	−0.669	<0.0001	−0.055	0.687
NH_4 (µmol ml^{-1})	0.292	0.028	0.330	0.012	−0.061	0.653
NO_x (µmol ml^{-1})	−0.718	<0.0001	−0.681	<0.0001	−0.027	0.842
NO_2 (µmol ml^{-1})	0.904	<0.0001	0.882	<0.0001	−0.010	0.461
TP (µmol ml^{-1})	−0.691	<0.0001	−0.658	<0.0001	−0.052	0.702
TN (µmol ml^{-1})	−0.697	<0.0001	−0.659	<0.0001	−0.023	0.862

as crescent, long, kinetoplastid, donut, bean, split, tiny, round and miscellaneous (see Fig. 2). Round and miscellaneous made up the majority of nuclei at all depths, but became less dominant in deeper samples due to an increase in the relative abundance of the split morphotype (Figs. 3 & 4). The split morphotype was remarkably constant in absolute abundance throughout the water column from 100 to 5000 m, which consequently increased their relative abundance from 0.07 % of total CARD-FISH eukaryotes in the lower euphotic zone (100 m) to 24 % in deep water masses (3500–5000 m) (Fig. 4).

Automated counts of prokaryotes using DAPI staining showed that prokaryotic abundance correlates negatively with depth ($r = -0.734$, $p < 0.0001$, $n = 59$), positively with total flagellate abundance ($r = 0.630$, $p < 0.0001$, $n = 59$), and positively with kinetoplastid abundance ($r = 0.338$, $p = 0.0089$, $n = 59$), but not with split nucleus abundance ($r = 0.065$, $p = 0.627$, $n = 59$). Image analysis of the size of DAPI signals on these filters showed a continuum, with no clear demarcation between prokaryotes and eukaryotic nuclei, rendering a cutoff based on size arbitrary (Fig. 5).

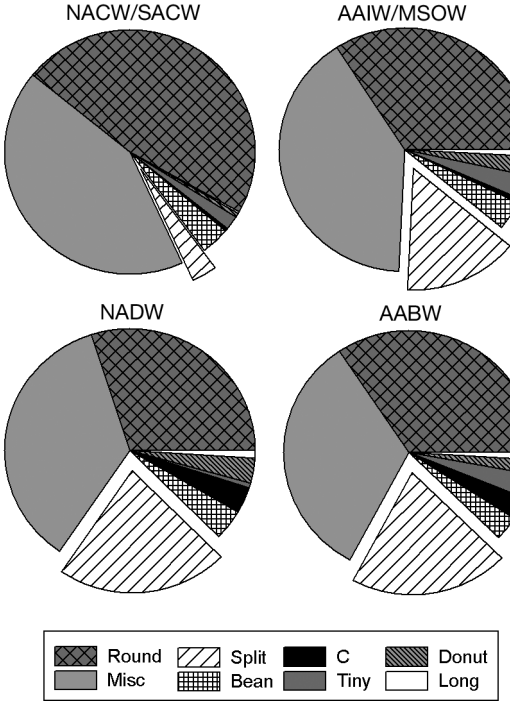

Fig 4. Relative abundance (percent of total CARD-FISH eukaryotes) of morphotypes (see Fig. 2 for details) in various water masses. Note the increase in the split morphotype with increasing depth, which is due to a constant absolute abundance of this morphotype as total eukaryotes declined. NACW/SACW: North/South Atlantic Central Water (samples taken between 250 and 500 m depth), AAIW/MSOW: Antarctic Intermediate Water/Mediterranean Sea Outflow Water (samples taken between 750 and 1000 m), NADW: North Atlantic Deep Water (samples taken between 2400 and 2750 m), AABW: Antarctic Bottom Water (samples taken between 3500 and 5000 m). Sample depth varied in order to target the center of each water mass. C: crescent; CARD-FISH: catalyzed reporter deposition fluorescence *in situ* hybridization

DISCUSSION

Protist abundance decreased exponentially from 100 to 900 m, then did not decrease further between 900 and 5000 m. This result is consistent with previous studies which have shown low but relatively stable numbers for heterotrophic nanoflagellates (the primary eukaryotes in deep-sea samples) below 1000 m (Fig. 6 in Sohrin et al. 2010). Using picoplankton and virus-like particle abundances from the same expedition (Parada et al. 2007), eukaryote abundances decrease by more than 2 orders of magnitude over the depths sampled, compared to one order of magnitude for picoplankton, and less than one for virus-like particles (Fig. 3). This suggests that viruses are relatively more important and small eukaryotes less important in the control of bacterial numbers in the bathypelagic region than in surface waters, which is also consistent with the conclusions reached by Aristegui et al. (2009).

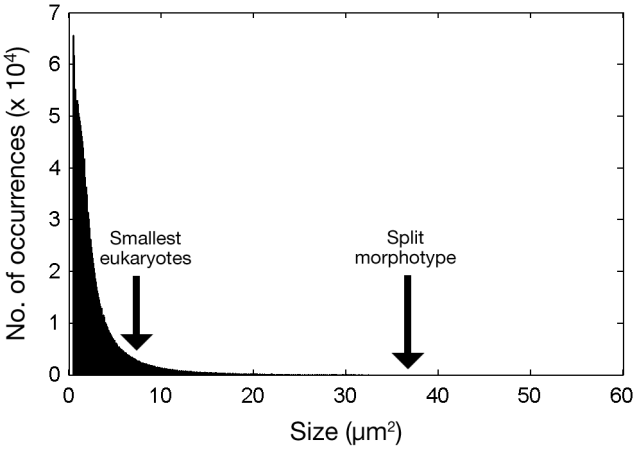

Fig 5. Frequency distribution of size of DAPI signals (total number of occurrences = 1 995 252) on 0.2 µm filters. Measurements were made using the automated microscope and Image-Pro Plus image analysis software. At least 100 random fields per filter from 60 filters (total fields = 6502) representing all stations and depths sampled were analyzed. The size of nuclei of 2 eukaryotic microbes (i.e. tiny and split morphotypes, arrows) demonstrates the size overlap between prokaryotes and eukaryotes

Counts obtained using FITC staining were higher than those using CARD-FISH for all samples. There are several possible reasons for this discrepancy, and we tested for such effects including loss of material from filters during the hybridization process, rough handling of filters, depressurization of samples, and the robotic scanning process of the microscope. Other factors that we were not able to test directly include eukaryotes which have too few copies of rRNA to show a positive CARD-FISH signal, which may be due to low activity levels of living cells (i.e. CARD-FISH could undercount) or to faster degradation of rRNA compared to the proteins and DNA which bind DAPI and FITC in dead cells. Conversely, a source of error in the DAPI-FITC counts could be the inclusion of a small fraction of prokaryotes in the tally that appear like eukaryotes because of very thick cell walls and DNA concentrated inside a nucleoid. Given the much higher abundance of prokaryotes in the samples, even the inclusion of a very small percentage of prokaryotes could make a big difference (Fig. 5). Although the scanning process of the robotic microscope introduced a significant error into counts of our samples (Table 3), it is nonetheless a useful tool for the quantification of very rare events, where the errors in manual counting would be at least as high due to the large number of empty fields to be assessed. By comparison, our counts of eukaryote abundances using the DAPI-FITC protocol are very similar to those of other workers despite the fact that they were collected at many different locations ranging from the Pacific (Sohrin et al. 2010) to the Mediterranean (Tanaka & Rassoulzadegan 2002). These data suggest that differences in the abundances of eukaryotic microbes do not primarily arise among ocean basins but are rather due to latitudinal differences (Sohrin et al. 2010) and due to different methodology employed (Table 5 in Nagata et al. 2010).

In our samples, depressurization pre- versus post-fixation did not significantly affect the number of eukaryotes counted by CARD-FISH in deep-sea samples. This finding is consistent with previous work, which has shown that many eukaryotes can be isolated from the deep sea after depressurization (Atkins et al. 1998, Arndt et al. 2003) and that eukaryotes cultured under pressure can survive and continue dividing after repeated depressurization (Turley et al. 1988). It is also consistent with the finding that protists do not burst due to intracellular bubble formation during pressure loss, and have nearly 100% survival when samples are depressurized over 0.5 to 1 h (Hemmingsen & Hemmingsen 1979). This validates the common practice of collecting samples for protist counts in non-pressurized samplers such as Niskin bottles, which allow for collection of the large volumes of water necessary for accurate counts, but do not maintain these samples at *in situ* pressure. It is important to emphasize, however, that while cells may not disappear due to depressurization, their physiology may be greatly impacted by changes in pressure. Any measurements to that effect (e.g. respiration, growth, feeding) may thus need to be performed under *in situ* pressure and temperature to obtain accurate results.

We used nuclear morphology to quantify certain types of organisms without knowing their taxonomic affiliation. The most striking example of this was the split morphotype (Fig. 2), in which the nucleus appears divided into 2 equal halves, which could be due to a double nucleus such as that found in the diplomonads (Lee et al. 2000; our Fig. 2) or possibly some feature of the cell blocking the center of the nucleus from view. These organisms were distinctive in the size, shape, and the relative brightness of their nucleus as viewed with DAPI staining and they readily hybridized with the EUK516 probe but not with KIN516. In individual deep-sea samples, the split nucleus type sometimes made up more than 50% of positive organisms using the EUK516 probe and robotic counting method, thus making this morphotype the most abundant in the deep sea where we sampled (Fig. 3). It showed no correlation with prokaryotic abundance, which was strongly correlated with depth while the split nucleus remained constant over the depth range sampled. The high abundance and consistent appearance of the nucleus mean that it would be impossible for the cells to be arranged on the filter in random orientations and we therefore propose that these organisms have cells which are flattened or are otherwise forced to land on the filter in a consistent orientation, similar to what we observed in diplomonads (Fig. 2).

We have not yet resolved the taxonomic affiliation of the split nucleus organism. It appears most similar to the twin nuclei of diplomonads, though it does not match precisely with the shape of the nuclei of cultured *Hexamita pusilla* ATTC #50336 or *Trepomonas agilis* ATTC #50337 (Fig. 2). Interestingly, the appearance of split nucleus type from our ocean samples had much less variation in appearance than that found in monocultures of both *Hexamita* and *Trepomonas* (Fig. 2). As we suspect for the split-nucleus type, *Hexamita* and *Trepomonas* are dorso-ventrally flattened and come to rest on the filter surface at a preferred orientation exposing their peculiar 2-

nucleus feature to view in the majority of individuals counted in our test (65.6% in *Hexamita*, 81.5% in *Trepomonas*). Most diplomonads are parasitic or live in anoxic, high nutrient environments (Lee et al. 2000), which makes them unlikely candidates for the most abundant eukaryote in the oxygenated, oligotrophic deep sea. However, microenvironments with anoxic and high-nutrient conditions exist in marine snow particles (Alldredge & Cohen 1987), which could provide a niche for diplomonads in the deep sea. Diplomonads are not currently known to exist in the deep sea, and are not to be confused with the diplonemids, reported to be very diverse in deep water (Lara et al. 2009).

Our examination of community composition based on nuclear morphotype shows that distinctive shifts occur between shallow and deep water samples, which independently validates the observations by Countway et al. (2007) based on 18S rRNA sequences. The abundance of organisms with recognizable nuclear morphologies means that a simple DAPI stain and visual inspection of a filter can be used as a first rough assessment of its eukaryotic community, allowing rapid characterization of some eukaryote types without FISH or sequencing. Classifying organisms based on morphology, including that of the nucleus, is an important tool of classical protist ecology. For example, the permanently condensed chromosomes typical of dinoflagellates and *Diplonema* have long been used to recognize these organisms (Lee et al. 2000, Lukeš et al. 2009). Given the abundance of the unusual split morphotype in our samples, we suggest that this simple tool can be used as a first step in the classification of some morphologically identifiable organisms from environmental samples prior to molecular characterization.

No correlation was found between eukaryote abundance by CARD-FISH and geographical factors such as latitude, longitude, or distance to nearest land, which may affect organic carbon input to the deep sea (Rowe 1983; our Table 4). This suggests a decoupling between surface water conditions and eukaryote abundance in the deep water. This decoupling may be due to the disconnect between the upper water masses with wind-driven circulation and the deep waters where thermohaline circulation dominates. In this data set, however, the apparent decoupling may also be due to the high between-sample variability and statistical type II errors, which are an inherent problem with any quantification of rare events. Some of the high between-sample variability (Table 4, Fig. 3) may also be attributable to the presence of aggregates in the deep sea. Recently, Bochdansky et al. (2010) found that macroscopic aggregates are found in increased numbers in some layers of the deep sea, particularly below 2000 m. If protists of the deep sea are primarily located on aggregates because numbers of freely-suspended prey items fall below threshold feeding levels (Wikner & Hagström 1991), much of the observed variability may be the result of this spatial heterogeneity.

Using the 6 supergroups proposed by Adl et al. (2005), Not et al. (2007) found the dominant eukaryotes in the deep Sargasso Sea to be Chromalveolata and Rhizaria, represented primarily by alveolate and radiolarian sequences, respectively. Another study in the Sargasso Sea found Chromalveolata and Rhizaria to dominate as well, but also found the supergroup Excavata represented by euglenozoan sequences (Countway et al. 2007). The taxonomic details within the euglenozoan sequences in that study were unclear, but Euglenazoa includes the kinetoplastids which we found to be numerically important in our deep-sea samples, as well as the diplonemids which have recently been discovered to be highly diverse in the deep sea (Lara et al. 2009). More studies using FISH probes targeted at apparently abundant groups such as the alveolates and radiolarians need to be undertaken on deep-sea samples to establish whether these groups are actually the dominant deep-sea eukaryotes or if biases inherent in PCR-based methods have led to this conclusion.

The kinetoplastids should be included in any future quantification of eukaryotes from the deep ocean, and care must be taken to include them in studies using molecular techniques. In water mass averages of our samples, their contribution to total CARD-FISH eukaryotes ranged from 15.9 to 27.1%. Kinetoplastids are a diverse branch of the eukaryotic tree (Simpson et al. 2006), and are as important in deep waters as in surface waters and sediments (Atkins et al. 2000, Arndt et al. 2003, Bochdansky & Huang 2010). Some kinetoplastids such as *Bodo* are barotolerant (Turley et al. 1988) or even barophilic (Turley & Carstens 1991). They have been collected from both the water column and sediments of the deep sea and successfully cultured in pressure vessels (Patterson et al. 1993). The kinetoplastids *Neobodo saliens* (formerly *Bodo saliens,* Simpson et al. 2006) and *Rhynchomonas nasuta* as well as an unknown kinetoplastid have been isolated from deep-sea hot vent sites (Atkins et al. 1998, 2000). Kinetoplastids have generally not been recorded specifically in sequences from the deep sea, but they are part of the Euglenozoa, whose sequences are

more abundant in deep water than in the euphotic zone (Countway et al. 2007). Kinetoplastids and euglenids, both members of the Euglenozoa, have also been found to be abundant in live counts and enrichment cultures from the deep sea (Arndt et al. 2003). Also, the recent discovery that diplonemids, another member of the Euglenozoa, are highly diverse in the deep sea (Lara et al. 2009) suggests that deep branches of the eukaryotic tree comprise a significant portion of deep-sea eukaryotes.

Acknowledgements. We thank Thomas Geer (Olympus America) and Don Laferty (Objective Imaging) for design of the robotic microscope and customized software development, Herman Boekel for the design and construction of the high-pressure chambers, and the crew of the RV 'Pelagia'. Fred Dobbs provided editorial comments. This project was supported by NSF grants No. 0550184 and No. 0826659 to A.B.B. and a grant of the Earth and Life Science Division of the Dutch Science Foundation (ARCHIMEDES project, 835.20.023) to G.J.H.

LITERATURE CITED

Adl SM, Simpson AG, Farmer MA, Andersen RA and others (2005) The new higher level classification of eukaryotes with emphasis on the taxonomy of protists. J Eukaryot Microbiol 52:399–451

Alldredge AL, Cohen Y (1987) Can microscale chemical patches persist in the sea? Microelectrode study of marine snow, fecal pellets. Science 235:689–691

Amann RI, Binder BJ, Olson RJ, Chisholm SW, Devereux R, Stahl DA (1990) Combination of 16S ribosomal-RNA-targeted oligonucleotide probes with flow-cytometry for analyzing mixed microbial-populations. Appl Environ Microbiol 56:1919–1925

Andersen P, Fenchel T (1985) Bacterivory by microheterotrophic flagellates in seawater samples. Limnol Oceanogr 30:198–202

Aristegui J, Gasol JM, Duarte CM, Herndl GJ (2009) Microbial oceanography of the dark ocean's pelagic realm. Limnol Oceanogr 54:1501–1529

Arndt H, Hausmann K, Wolf M (2003) Deep-sea heterotrophic nanoflagellates of the Eastern Mediterranean Sea: qualitative and quantitative aspects of their pelagic and benthic occurrence. Mar Ecol Prog Ser 256:45–56

Atkins MS, Anderson OR, Wirsen CO (1998) Effect of hydrostatic pressure on the growth rates and encystment of flagellated protozoa isolated from a deep-sea hydrothermal vent and a deep shelf. Mar Ecol Prog Ser 171:85–95

Atkins MS, Teske AP, Anderson OR (2000) A survey of flagellate diversity at four deep-sea hydrothermal vents in the Eastern Pacific Ocean using structural and molecular approaches. J Eukaryot Microbiol 47:400–411

Beardsley C, Knittell K, Amann R, Pernthaler J (2005) Quantification and distinction of aplastidic and plastidic marine nanoplankton by fluorescence *in situ* hybridization. Aquat Microb Ecol 41:163–169

Bochdansky AB, Huang L (2010) Re-evaluation of the EUK516 probe for the domain Eukarya results in a suitable probe for the detection of kinetoplastids, an important group of parasitic and free-living flagellates. J Eukaryot Microbiol 57:229–235

Bochdansky AB, van Aken HM, Herndl GJ (2010) Role of macroscopic particles in deep-sea oxygen consumption. Proc Natl Acad Sci USA 107:8287–8291

Countway PD, Gast RJ, Dennett MR, Rose JM, Caron DA (2007) Distinct protistan assemblages characterize the euphotic zone and deep sea (2500 m) of the western North Atlantic (Sargasso Sea and Gulf Stream). Environ Microbiol 9:1219–1232

Edgcomb V, Orsi W, Bunge J, Jeon S and others (2011) Protistan microbial observatory in the Cariaco Basin, Caribbean. I. Pyrosequencing vs Sanger insights into species richness. ISME J 5:1344–1356

Fenchel T (1986) The ecology of heterotrophic microflagellates. Adv Microb Ecol 9:57–97

Fukuda H, Sohrin R, Nagata T, Koike I (2007) Size distribution and biomass of nanoflagellates in meso- and bathypelagic layers of the subarctic Pacific. Aquat Microb Ecol 46:203–207

Gasol JM, Vaque D (1993) Lack of coupling between heterotrophic nanoflagellates and bacteria — a general phenomenon across aquatic systems. Limnol Oceanogr 38: 657–665

Hemmingsen EA, Hemmingsen BB (1979) Lack of intracellular bubble formation in microorganisms at very high gas supersaturations. J Appl Physiol 47:1270–1277

Lara E, Moreira D, Vereshchaka A, López-Garcia P (2009) Pan-oceanic distribution of new highly diverse clades of deep-sea diplonemids. Environ Microbiol 11:47–55

Lee JJ, Leedale GF, Bradbury P (eds) (2000) Society of protozoologists. Illustrated Guide to the Protozoa, 2nd edn. Allen Press, Lawrence, KS

Lukeš J, Leander BS, Keeling BJ (2009) Cascades of convergent evolution: the corresponding evolutionary histories of euglenozoans and dinoflagellates. Proc Natl Acad Sci USA 106:9963–9970

Nagata T, Tamburini C, Arístegui J, Baltar F and others (2010) Emerging concepts on microbial processes in the bathypelagic ocean — ecology, biogeochemistry, and genomics. Deep-Sea Res II 57:1519–1536

Not F, Gausling R, Azam F, Heidelberg JF, Worden AZ (2007) Vertical distribution of picoeukaryotic diversity in the Sargasso Sea. Environ Microbiol 9:1233–1252

Paffenhöfer GA, Tzeng M, Hristov R, Smith CL, Mazzocchi MG (2003) Abundance and distribution of nanoplankton in the epipelagic subtropical/tropical open Atlantic Ocean. J Plankton Res 25:1535–1549

Parada V, Sintes E, van Aken H, Weinbauer MG, Herndl GJ (2007) Viral abundance, decay, and diversity in the meso- and bathypelagic waters of the North Atlantic. Appl Environ Microbiol 73:4429–4438

Patterson DJ, Nygaard K, Steinberg G, Turley CM (1993) Heterotrophic flagellates and other protists associated with oceanic detritus throughout the water column in the mid North-Atlantic. J Mar Biol Assoc UK 73:67–95

Pernthaler A, Pernthaler J, Amann R (2002) Fluorescence *in situ* hybridization and catalyzed reporter deposition for the identification of marine bacteria. Appl Environ Microbiol 68:3094–3101

Rowe GT (1983) Biomass and production of the deep-sea macrobenthos. In: Rowe, GT (ed) The sea, Vol 8. John Wiley & Sons, New York, NY

Sherr B, Sherr E (1983) Enumeration of heterotrophic micro-

protozoa by epifluorescence microscopy. Estuar Coast Shelf Sci 16:1–7

Simpson AGB, Stevens JR, Lukeš J (2006) The evolution and diversity of kinetoplastid flagellates. Trends Parasitol 22: 168–174

Sohrin R, Imazawa M, Fukuda H, Suzuki Y (2010) Full-depth profiles of prokaryotes, heterotrophic nanoflagellates, and ciliates along a transect from the equatorial to the subarctic central Pacific Ocean. Deep-Sea Res II 57: 1537–1550

Tanaka T, Rassoulzadegan F (2002) Full-depth profile (0–2000 m) of bacteria, heterotrophic nanoflagellates and ciliates in the NW Mediterranean Sea: vertical partitioning of microbial trophic structure. Deep-Sea Res II 49: 2093–2107

Teira E, Reinthaler T, Pernthaler A, Pernthaler J, Herndl GJ (2004) Combining catalyzed reporter deposition-fluorescence *in situ* hybridization and microautoradiography to detect substrate utilization by bacteria and archaea in the deep ocean. Appl Environ Microbiol 70:4411–4414

Tomczak M, Godfrey JS (2003) Regional oceanography: an introduction, 2nd edn. Butterworth-Heinemann, Boston, MA

Turley CM, Carstens M (1991) Pressure tolerance of oceanic flagellates — implications for remineralization of organic-matter. Deep-Sea Res Part A 38: 403–413

Turley CM, Lochte K, Patterson DJ (1988) A barophilic flagellate isolated from 4500 m in the mid-North Atlantic. Deep-Sea Res Part A 35:1079–1092

Wikner J, Hagström Å (1991) Annual study of bacterioplankton community dynamics. Limnol Oceanogr 36: 1313–1324

Editorial responsibility: Josep Gasol, Barcelona, Spain

Submitted: November 23, 2010; Accepted: August 29, 2011
Proofs received from author(s): November 18, 2011